Gyrokinetic Simulations of Solar Wind Turbulence from Ion to Electron Scales

G. G. Howes,[1,2,*] J. M. TenBarge,[1] W. Dorland,[3,2] E. Quataert,[4]
A. A. Schekochihin,[5,2] R. Numata,[3,2] and T. Tatsuno[3]

[1]*Department of Physics and Astronomy, University of Iowa, Iowa City, Iowa 52242, USA.*
[2]*Isaac Newton Institute for Mathematical Sciences, Cambridge, CB3 0EH, U.K.*
[3]*Department of Physics, University of Maryland, College Park, Maryland 20742-3511, USA.*
[4]*Department of Astronomy, University of California, Berkeley, California 94720, USA.*
[5]*Rudolf Peierls Centre for Theoretical Physics, University of Oxford, Oxford, OX1 3NP, U.K.*

(Dated: January 19, 2013)

The first three-dimensional, nonlinear gyrokinetic simulation of plasma turbulence resolving scales from the ion to electron gyroradius with a realistic mass ratio is presented, where all damping is provided by resolved physical mechanisms. The resulting energy spectra are quantitatively consistent with a magnetic power spectrum scaling of $k^{-2.8}$ as observed in *in situ* spacecraft measurements of the "dissipation range" of solar wind turbulence. Despite the strongly nonlinear nature of the turbulence, the linear kinetic Alfvén wave mode quantitatively describes the polarization of the turbulent fluctuations. The collisional ion heating is measured at sub-ion-Larmor radius scales, which provides the first evidence of the ion entropy cascade in an electromagnetic turbulence simulation.

Introduction.—Although studies of the inertial range of magnetized plasma turbulence date back more than four decades [1], only recently has the "dissipation range"—the kinetic scales from the ion to the electron Larmor radius and beyond—become a focus of the astrophysics and heliospheric physics communities. The dynamics in the dissipation range is critical to a fundamental understanding of plasma turbulence because it is at these scales that the turbulence is dissipated and the turbulent energy is converted into ion and electron thermal energy. One of the principal challenges is that the dynamics at these scales is weakly collisional in most diffuse space and astrophysical plasmas. Therefore, a kinetic description of the plasma dynamics and energy conversion via wave-particle interactions is necessary [2–4]. This is significantly more challenging than the fluid descriptions, such as magnetohydrodynamics (MHD), commonly used in the study of the inertial-range turbulence. To enable direct comparisons of numerical results to observations of the dissipation range, one must cover a meaningful dynamic range while satisfying three important conditions: the turbulence must be modeled in three spatial dimensions [5], kinetic dissipation mechanisms must be resolved, and a realistic mass ratio must be used.

Early observational studies of the solar wind probed little more than a decade in satellite-frame frequency above the spectral break marking the onset of the dissipation range [6]. More recent, better resolved measurements show that the one-dimensional magnetic energy spectrum typically exhibits a power-law behavior with a $-5/3$ spectral index at low frequencies, a break at a few tenths of a Hz, and a steeper apparent power-law spectrum at higher frequencies. The spectral exponent in this high-frequency range reported in most recent studies ranges from -2.6 to -2.8 [7–11]. Ideas proposed to explain the steeper dissipation range spectrum include proton cyclotron damping [1], Landau damping of kinetic Alfvén waves [3, 6], and the dispersion of whistler waves [12].

Following modern theories of anisotropic MHD turbulence [13], a theoretical picture of the kinetic turbulent cascade was developed [4, 14, 15] that proposed an inertial range containing an anisotropic cascade of MHD Alfvén waves at $k_\perp \rho_i \ll 1$, a break in the magnetic energy spectrum at the perpendicular scale of the ion Larmor radius $k_\perp \rho_i \sim 1$, and a dissipation range of kinetic Alfvén waves (KAWs) at $k_\perp \rho_i \gg 1$. Because of the spatial anisotropy of the fluctuations ($k_\perp \gg k_\parallel$), the turbulent fluctuation frequencies stay well below the ion cyclotron frequency, $\omega \ll \Omega_i$, in both the inertial and dissipation ranges. At scales $k_\perp \rho_i \gtrsim 1$, collisionless damping via the Landau resonance with ions and electrons dissipates the turbulence. Numerical evidence that this picture yields observationally sensible predictions was provided by the first fully electromagnetic, 3D, kinetic simulations of turbulence over the range $0.4 \leq k_\perp \rho_i \leq 8$ [16] using the gyrokinetic equations [4, 17, 18], which are a rigorous low-frequency anisotropic limit of kinetic theory.

Over the past two years, a number of observational studies have broken exciting new ground by probing the dynamics of solar wind turbulence up to satellite-frame frequencies $f \sim 100$ Hz [7–11]. All of these observations clearly demonstrate a nearly power-law behavior of the magnetic power spectrum over the dissipation range, 1 Hz $\lesssim f \lesssim$ 50 Hz. This finding is in disagreement with cascade models of KAW turbulence that employed linear Landau damping rates and predicted that the latter would be sufficient to lead to an exponential fall-off of the spectrum before it reached the electron scales [3, 19]. This raises the important question of whether the KAW cascade can explain the observed spectra. Other measurements are consistent with the key assumptions of KAW turbulence models: the turbulence remains anisotropic on these scales [10, 11, 20]; and the

fluctuations appear consistent with a KAW-like polarization [7, 11] (see, however, [10]).

This Letter presents the first nonlinear gyrokinetic simulation of solar wind turbulence resolving the entire range of scales from the ion (proton) to the electron Larmor radius with the correct mass ratio. The significant advance achieved by this simulation is that no artificial dissipation is required to remove energy at small scales; all dissipation is due to resolved collisionless damping via the Landau resonances. The steady-state spectra may therefore be compared directly to observations of the solar wind dissipation range [21]. The resulting numerical spectra are quantitatively consistent with the recent *in situ* satellite observations [7–9, 11], demonstrating that a KAW cascade, even when the physical damping mechanisms are taken into account, can produce a nearly power-law behavior over the dissipation range.

Simulation.—The simulation in this paper was performed using `AstroGK`, the Astrophysical Gyrokinetics Code, developed specifically to study kinetic turbulence in astrophysical plasmas. A detailed description of the code and the results of linear and nonlinear benchmarks are presented in [22], so we give here only a brief overview.

`AstroGK` evolves the perturbed gyroaveraged distribution function $h_s(x, y, z, \lambda, \varepsilon)$ for each species s, the scalar potential φ, parallel vector potential $A_\parallel$, and the parallel magnetic field perturbation $\delta B_\parallel$ according to the gyrokinetic equation and the gyroaveraged Maxwell's equations [17, 18]. The velocity space coordinates are $\lambda = v_\perp^2/v^2$ and $\varepsilon = v^2/2$. The domain is a periodic box of size $L_\perp^2 \times L_\parallel$, elongated along the straight, uniform mean magnetic field B_0. Note that, in the gyrokinetic formalism, all quantities may be rescaled to any parallel dimension satisfying $L_\parallel/L_\perp \gg 1$. Uniform Maxwellian equilibria for ions (protons) and electrons are chosen, and the correct mass ratio $m_i/m_e = 1836$ is used. Spatial dimensions (x, y) perpendicular to the mean field are treated pseudospectrally; an upwind finite-difference scheme is used in the parallel direction, z. Collisions are incorporated using a fully conservative, linearized collision operator that includes energy diffusion and pitch-angle scattering [23, 24].

Because turbulence in astrophysical plasmas exists over a wide range of scales—for example, in the near-Earth solar wind, the driving scale is $L \sim 10^6$ km and the electron Larmor radius is $\rho_e \sim 1$ km [3]—numerical simulations are necessarily limited to modeling only a portion of the turbulent cascade. Two key challenges in the kinetic simulation of turbulence are modeling the energy injection at the largest scales and removing the turbulent energy at the smallest resolved scales.

In gyrokinetic simulations using `AstroGK`, the simulation domain is much smaller than the physical driving scale, and covers scales at which the turbulent fluctuations are sufficiently anisotropic ($k_\perp \gg k_\parallel$) for the gyrokinetic approximation to be well satisfied [3, 4, 18]; this assumption of anisotropy is consistent with recent multipoint spacecraft measurements [10, 11]. In the simulation reported here, nonlinear energy transfer from turbulent fluctuations at scales larger than the largest scales in our domain ($k_{\perp 0}\rho_i = 1$) is modeled using six modes of a parallel "antenna" current $j^a_{\parallel,\mathbf{k}}$ added via Ampère's Law [22]. These driven modes have wavevectors $(k_x\rho_i, k_y\rho_i, k_z L_\parallel/2\pi) = (1, 0, \pm 1), (0, 1, \pm 1), (-1, 0, \pm 1)$, frequencies $\omega_a = 1.14\omega_{A0}$ (where $\omega_{A0} \equiv k_{\parallel 0} v_A$ is a characteristic Alfvén frequency corresponding to the parallel size $L_\parallel$ of the domain), and amplitudes that evolve according to a Langevin equation. This produces Alfvénic wave modes with a frequency $\omega \sim \pm k_{\parallel 0} v_A$ and a decorrelation rate comparable to ω, as expected for critically balanced Alfvénic turbulence [13]. Note that energy is injected only at $k_\perp \rho_i = 1$, so the amplitudes at all higher $k_\perp$ are determined by the nonlinear dynamics.

The key advance achieved here is resolving a fully dealiased range with a perpendicular scale separation of $\sqrt{m_i/m_e} \simeq 42.8$. This spans from the proton Larmor radius at $k_\perp \rho_i = 1$ to the electron Larmor radius at $k_\perp \rho_e = 1$ (or $k_\perp \rho_i \simeq 42.8$ for $T_i/T_e = 1$). Wave-particle interactions via the Landau resonance are resolved and sufficient to damp the electromagnetic fluctuations within the simulated range of scales. The energy spectra at all scales, including the dissipative scales, are shaped by resolved physical processes, and so may be directly compared to observational data. This would not be possible with standard fluid or hybrid approaches, such as Hall MHD or kinetic ion-fluid electron models, because the bulk of the damping of the electron motion in such models is typically governed by an *ad hoc* fluid model of the damping, such as viscosity or resistivity [25].

The simulation domain size is $L_\perp = 2\pi\rho_i$ with dimensions $(n_x, n_y, n_z, n_\lambda, n_\varepsilon, n_s) = (128, 128, 128, 64, 16, 2)$. The plasma parameters are $\beta_i = 1$ and $T_i/T_e = 1$. In kinetic turbulence simulations, the inclusion of sufficient collisionality is essential to prevent the small-scale structure in velocity space generated by wave-particle interactions from exceeding the velocity space resolution. For this reason, collision frequencies of $\nu_i = 0.04\omega_{A0}$ and $\nu_e = 0.5\omega_{A0}$ have been chosen carefully to achieve sufficient damping of small-scale velocity-space structure yet to avoid altering the collisionless dynamics of each species over the range of scales at which the kinetic damping is non-negligible. A recursive expansion procedure [15] is used to reach a statistically steady state at acceptable numerical cost. At low spatial resolution, the simulation is run for more than an outer-scale eddy turnover time (this turnover time is $\tau_0 = 5.52\omega_{A0}^{-1}$) to reach a steady state. Resolution in each spatial dimension is then doubled, and the simulation is run to a new steady state, which requires only a time of order the cascade time at the smallest mode before expansion. This simulation has been evolved, using this recursive procedure, to a time of

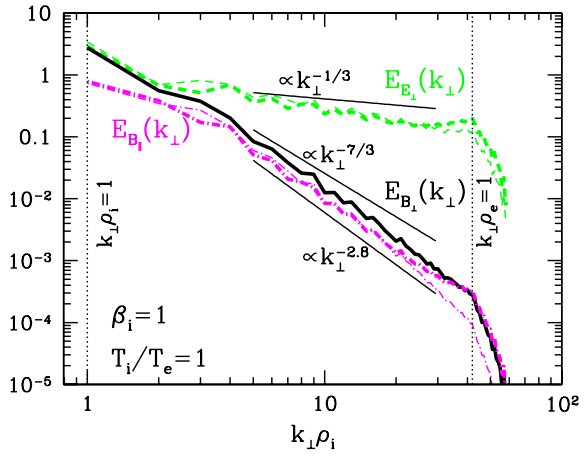

FIG. 1. For a $\beta_i = 1$ and $T_i/T_e = 1$ plasma, thick lines are numerical energy spectra for the perpendicular magnetic (solid), electric (dashed), and parallel magnetic (dot-dashed) field perturbations. Thin lines are the perpendicular electric (dashed) and parallel magnetic (dot-dashed) energy spectra predicted from the perpendicular magnetic energy spectrum in the simulation assuming the polarization of a linear collisionless KAW—the result is in excellent agreement with the simulation for $k_\perp\rho_i \lesssim 30$. Ion and electron Larmor radius scales are marked by vertical dotted lines.

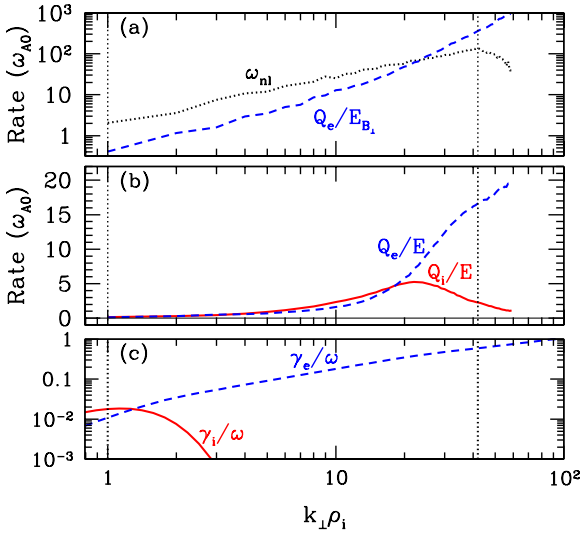

FIG. 2. (a) "Nonlinear damping rate" $Q_e/E_{B_\perp}$ and nonlinear transfer frequency ω_{nl} show strong damping for $k_\perp\rho_i \gtrsim 25$. (b) Ion (solid) and electron (dashed) collisional heating vs. $k_\perp$, normalized to generalized energy E [4]. (c) The linear ion (solid) and electron (dashed) Landau damping rates.

$t = 18.70\omega_{A0}^{-1}$.

Spectra.—In Fig. 1, steady-state energy spectra (thick lines) are presented, including the perpendicular magnetic (solid), parallel magnetic (dot-dashed), and perpendicular electric (dashed) energy spectra. Normalizations of the energy spectra are the same as in our previous work [16]. The salient feature of the perpendicular magnetic energy spectrum is its nearly power-law appearance over the entire range of scales from $k_\perp\rho_i = 1$ to $k_\perp\rho_e = 1$. For a KAW cascade, the theoretical prediction for its scaling in the absence of dissipation is $k_\perp^{-7/3}$ [3, 4]; the measured spectrum over the range $5 \le k_\perp\rho_i \le 30$ is slightly steeper, about $k_\perp^{-2.8}$, in remarkable agreement with recent observations [8, 9, 11]. This suggests that resolving the damping via the Landau resonance with electrons in this region is important to enable direct comparison to satellite observations. Clearly, the energy spectra of this gyrokinetic simulation do not exhibit an exponential falloff. It appears that the effect of (relatively weak) electron Landau damping is merely to steepen the spectra slightly. For a $\beta_i = 1$ plasma, the only propagating wave mode in gyrokinetics at these scales is the KAW, so this numerical result disproves by counterexample a recent claim [19] that the KAW cascade cannot reach scales of order the electron gyroradius $k_\perp\rho_e \sim 1$.

KAW Polarized Turbulence.—An important question in the study of plasma turbulence at small scales is whether linear wave properties can provide useful guidance in exploring the characteristics of the nonlinear fluctuations in a turbulent plasma. To investigate this question, we show in Fig. 1 the spectra for $E_{E_\perp}(k_\perp)$ (thin dashed) and $E_{\delta B_\parallel}(k_\perp)$ (thin dot-dashed), predicted from the numerical spectrum of $E_{B_\perp}(k_\perp)$ (thick solid) by assuming that the relationships between the different components of the fields are described by the linear eigenfunctions of the KAW derived from the linear collisionless gyrokinetic dispersion relation [18]. The predicted spectra are in excellent agreement with the numerical spectra for $E_{E_\perp}(k_\perp)$ (thick dashed) and $E_{\delta B_\parallel}(k_\perp)$ (thick dot-dashed) for scales $k_\perp\rho_i \lesssim 30$, giving strong support to the view that the linear wave properties of the kinetic plasma are crucial in determining the nature of the turbulent fluctuations. Note that recent measurements of solar wind turbulence have found consistency with KAW polarization [11]. Only for $k_\perp\rho_i \gtrsim 30$ does the nature of the fluctuations in our simulation deviate significantly from that of the linear collisionless KAW; this may be due to the effect of collisions (see Fig. 2).

We stress that while the relative polarization of the turbulent fluctuations follows the linear theory, this does *not* mean that the turbulence is weak—in fact, the $k_\perp^{-7/3}$ prediction comes from assuming a critically balanced, and therefore strong, KAW turbulence [3, 4], which means that the fluctuations decorrelate over a timescale comparable to the linear wave period.

Heating.—One of the fundamental goals in the study of the dissipation range of plasma turbulence is to identify the physical mechanisms by which the energy in turbulent fluctuations is converted into plasma heat. By Boltzmann's H theorem, the increase of entropy and associated irreversible heating in a kinetic plasma is possible only by the action of collisions [18]. Collisionless wave-

particle interactions transfer electromagnetic fluctuation energy to the perturbed particle distribution functions. It has been proposed that nonlinear phase mixing, due to the variation in the gyroaveraged $\mathbf{E}\times\mathbf{B}$ drift velocity at sub-Larmor radius scales, causes the non-thermal energy in the distribution function to undergo a phase-space cascade to smaller scales in both physical and velocity space, the so-called entropy cascade [4]. The entropy cascade ultimately enables irreversible thermodynamic heating in a weakly collisional plasma by driving the nonthermal energy to small scales in velocity space, where even weak collisions can act effectively. The Landau damping merely transfers energy from the electromagnetic fluctuations to the entropy cascade.

The gyrokinetic heating equations [18] have been implemented in `AstroGK` to diagnose the plasma collisional heating rate by species, Q_s. Dissipation of the KAW cascade by electron Landau damping in the simulation is sufficient to terminate the cascade, demonstrated in Fig. 2 (a) by comparing the "nonlinear damping rate" $\gamma_{nl}\sim Q_e/E_{B_\perp}$ (dashed) to the frequency of the nonlinear energy transfer $\omega_{nl}\sim k_\perp v_A(\delta B_\perp/B_0)(1+k_\perp^2\rho_i^2/2)^{1/2}$ [3] (dotted). Here $E_{B_\perp}$ is the perpendicular magnetic energy of the KAW cascade, spectra are summed in linearly spaced bins in $k_\perp$, and time is given in units of ω_{A0}^{-1}. A key result of this Letter, in Fig. 2 (b), is the ion (solid) and electron (dashed) collisional heating rate normalized to the generalized energy E (which includes energy from both KAW and ion entropy cascades) [4]. Also plotted (c) are the linear collisionless Landau damping rates for ions (solid) and electrons (dashed) in the gyrokinetic limit. Although the linear damping onto the ions peaks at $k_\perp\rho_i\sim 1$, the peak of the ion collisional heating occurs at the higher wavenumber of $k_\perp\rho_i\sim 20$. This shift of the peak of ion collisional heating to higher wavenumber is consistent with the predicted effect of the ion entropy cascade, which transfers energy to sub-Larmor scales. Our simulation results thus provide the first evidence of the ion entropy cascade in a 3D, driven, electromagnetic turbulence simulation, previously accomplished only for a 2D, decaying, electrostatic case [26].

Conclusions.—We have presented the first nonlinear kinetic simulation of solar wind turbulence resolving the entire range of scales from the ion (proton) to the electron Larmor radius with the correct mass ratio. No artificial dissipation was required to remove energy at the small scales; all dissipation was due to resolved collisionless damping mechanisms. The resulting steady-state energy spectra are quantitatively consistent with recent *in situ* satellite observations which demonstrate nearly power-law behavior over the dissipation range. Although the turbulence is strong, the relative polarizations of the electromagnetic fluctuations in this nonlinearly turbulent system are still quantitatively described by the linear kinetic Alfvén wave mode over much of the dissipation range. Although the collisionless ion damping of the electromagnetic fluctuations peaks at $k_\perp\rho_i\sim 1$, collisional ion heating in the numerical simulation peaks at a much higher wavenumber of $k_\perp\rho_i\sim 20$. This is consistent with the presence of the theoretically predicted ion entropy cascade [4], responsible for mediating entropy increase and irreversible thermodynamic heating in weakly collisional plasmas such as the solar wind. Future numerical and analytical studies of the kinetic Alfvén wave cascade and its dissipation will aim to determine quantitatively the plasma heating as a function of plasma parameters.

This work was supported by the DOE Center for Multiscale Plasma Dynamics, STFC, Leverhulme Trust Network for Magnetised Plasma Turbulence, NSF-DOE PHY-0812811, and NSF ATM-0752503. Computing resources were supplied through DOE INCITE 2008 Award PSS002, NSF TeraGrid 2009 Award PHY090084, and DOE INCITE Award FUS030.

* gregory-howes@uiowa.edu

[1] P. J. Coleman, Jr., Astrophys. J. **153**, 371 (1968).
[2] E. Marsch, Living Rev. Solar Phys. **3** (2006).
[3] G. G. Howes *et al.*, J. Geophys. Res. **113**, A05103 (2008).
[4] A. A. Schekochihin *et al.*, Astrophys. J. Supp. **182**, 310 (2009).
[5] Three spatial dimensions are required because the dominant $\mathbf{E}\times\mathbf{B}$ nonlinearity cannot exist unless both dimensions perpendicular to the mean field are included, while Alfvénic wave propagation requires the parallel dimension as well [4,18].
[6] R. J. Leamon *et al.*, J. Geophys. Res. **104**, 22331 (1999).
[7] F. Sahraoui, *et al.*, Phys. Rev. Lett. **102**, 231102 (2009).
[8] K. H. Kiyani *et al.*, Phys. Rev. Lett. **103**, 075006 (2009).
[9] O. Alexandrova *et al.*, Phys. Rev. Lett. **103**, 165003 (2009).
[10] C. H. K. Chen *et al.*, Phys. Rev. Lett. **104**, 255002 (2010).
[11] F. Sahraoui *et al.*, Phys. Rev. Lett. **105**, 131101 (2010).
[12] O. Stawicki *et al.*, J. Geophys. Res. **106**, 8273 (2001).
[13] P. Goldreich & S. Sridhar, Astrophys. J. **438**, 763 (1995).
[14] E. Quataert & A. Gruzinov, Astrophys. J. **520**, 248 (1999).
[15] G. G. Howes, Phys. Plasmas **15**, 055904 (2008).
[16] G. G. Howes *et al.*, Phys. Rev. Lett. **100**, 065004 (2008).
[17] E. A. Frieman & L. Chen, Phys. Fluids **25**, 502 (1982).
[18] G. G. Howes *et al.*, Astrophys. J. **651**, 590 (2006).
[19] J. J. Podesta *et al.*, Astrophys. J. **712**, 685 (2010).
[20] J. J. Podesta, Astrophys. J. **698**, 986 (2009).
[21] A Maxwellian equilibrium distribution is assumed, sothe generation of the firehose and mirror instabilities by temperature anisotropies [27] is not included.
[22] R. Numata *et al.*, J.Comp. Phys. **229**, 9347 (2010).
[23] I. G. Abel *et al.*, Phys. Plasmas **15**, 122509 (2008).
[24] M. Barnes *et al.*, Phys. Plasmas **16**, 072107 (2009).
[25] G. G. Howes *et al.*, Phys. Rev. Lett. **101**, 149502 (2008).
[26] T. Tatsuno *et al.*, Phys. Rev. Lett. **103**, 015003 (2009).
[27] S. D. Bale *et al.*, Phys. Rev. Lett. **103**, 211101 (2009).